Seismo-Acoustic Analysis of Debris Flows events at the Illgraben catchment, Switzerland

Giacomo Belli[1], Emanuele Marchetti[1], Fabian Walter[2], Brian, McArdell[3], and Michaela Wenner[2]

1. Department of Earth Sciences, University of Firenze, Firenze, Italy.
2. ETH, Laboratory of Hydraulics, Hydrology and Glaciology, 8093 Zürich, Switzerland.
3. WSL, Swiss Federal Institute for Forest, Snow and Landscape Research,
8903 Birmensdorf, Switzerland.

Instrumental setup

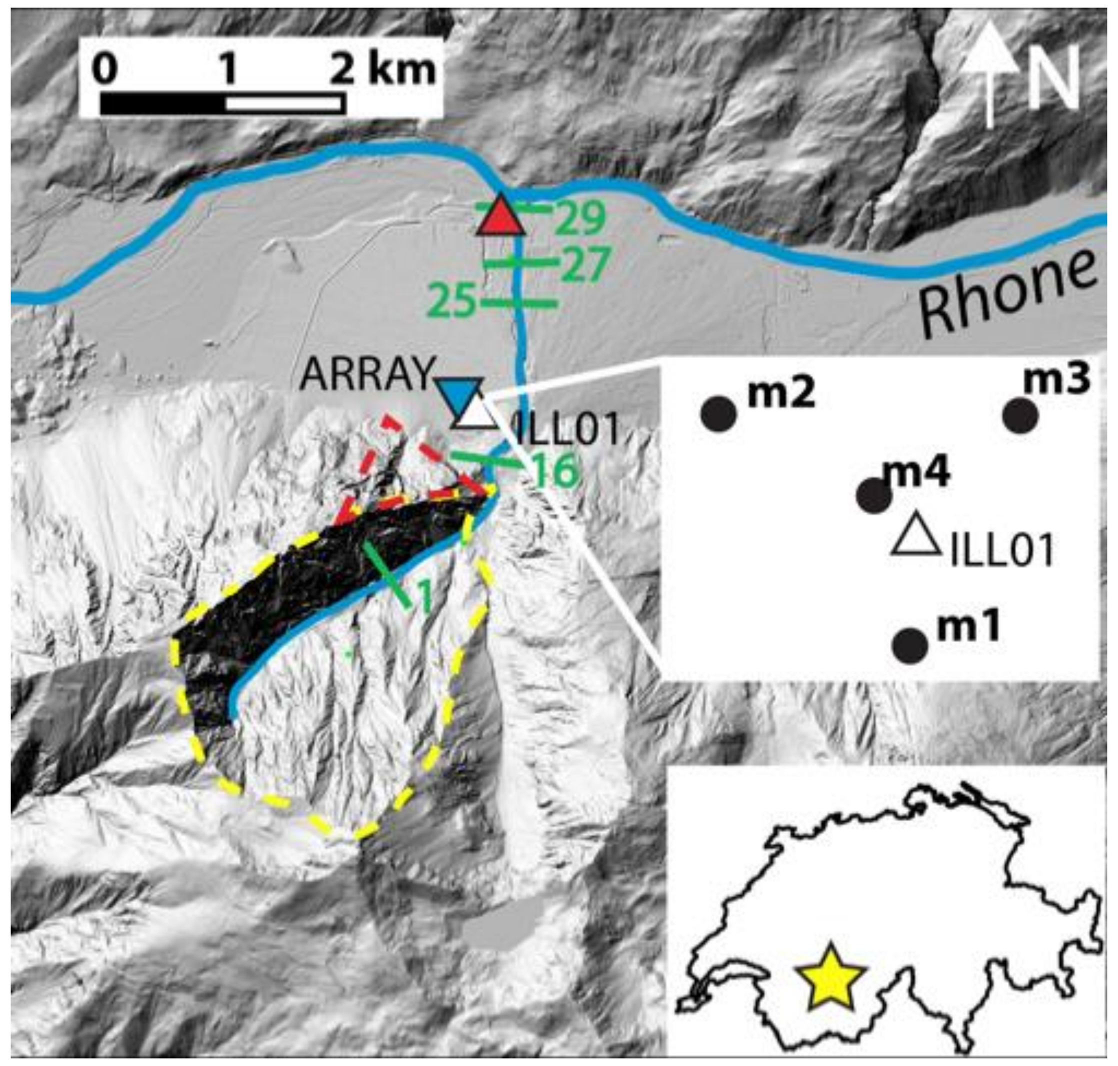

Figure 1: geographic setting of Illgraben

We present preliminary results of a seismo-acoustic study of debris-flow events at Illgraben (Switzerland) (Figure 1), in the 2017-2019 period. We combine seismo-acoustic data with hydraulic and physical measurements (WSL, Zurich), in order to achieve an improved understanding of the dynamics of the source mechanisms of the two wavefields. We used a small-aperture, 5 element, infrasonic array (@ 50 Hz) and seismic data were collected by a Lennartz LE3D 1s seismometer (@ 100 Hz).

Both the array (cyan triangle,) and the seismometer (ILL01) are deployed about 600 m north of the Illgraben catchment mouth (Figure 1). In the 2017-2019 period, 18 debris-flows events occurred (Table 1). Recorded debris-flow events are characterized by an extreme variability in size, duration and in the hydraulic and physical features (Table 1, Figure 2), suggesting a wide variability in flow dynamics, and reflecting differences in composition and water content.

Flow data

Table 1: hydraulic database of the Illgraben 2017-2019 debris-flow events (n.m. *not measured)*. Flow velocity is evaluated from the differences between arrival times at CD27(or CD28) and CD29. Flow depth reported values are measured at CD 29 with radar and laser altimeters.

Date	CD1 Arrival Time (UT)	Volume (m^3)	Velocity (m/s) (CD27-29)	Flow Depth (m) (CD29)	Bulk Density (Kg/m^3)	Seismic Signal	Infrasound Signal
2017/05/29	16:58:31	100000	6.67	4.8	n.m.	Clear	Clear
2017/06/03	23:27:38	9000	5.10	3.3	n.m.	Clear	Clear
2017/06/14	19:30:48	35000	7.20	3.4	n.m.	Clear	Clear
2018/06/11	10:46:39	n.m.	n.m.	n.m.	n.m.	Extremely Weak	Not Visible
2018/06/12	18:29:16	n. m.	n. m.	n. m.	n.m.	Extremely Weak	Not Visible
2018/07/25	16:56:40	n. m.	4.70	2.0	n.m.	Clear	Clear
2018/08/08	17:49:25	n. m.	6.69	n. m.	n.m.	Clear	Not Working
2019/06/10	17:02:51	3300	0.90	0.64	1640	Clear	Very Weak
2019/06/10	22:01:17	6600	2.38	0.59	1730	Weak	Very Weak
2019/06/20	09:12:17	n. m.	n. m.	n. m.	n.m.	Weak	Not Visible
2019/06/21	19:34:42	83000	5.60	2.45	1930	Clear	Clear
2019/07/01	23:00:29	n. m.	n. m.	n. m.	n.m.	Clear	Clear
2019/07/02	22:09:28	78000	3.80	1.62	2190	Clear	Clear
2019/07/03	16:43:15	n.m.	2.50	0.71	2340	Very Weak	Not Visible
2019/07/15	03:40:21	16000	5.00	0.68	2170	Clear	Weak
2019/07/26	17:33:12	64000	6.97	1.21	2240	Clear	Clear
2019/08/11	17:02:34	53000	5.56	n.m.	n.m.	Clear	Clear
2019/08/20	16:40:59	13000	0.95	0.89	1980	Clear	Weak

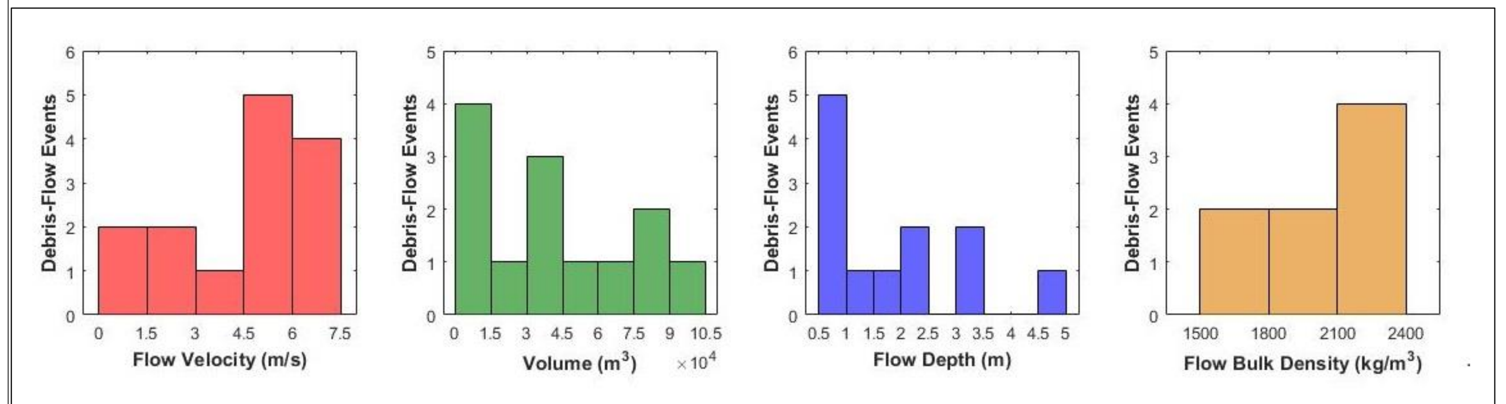

Figure 2: Illgraben 2017-2019 debris-flow events hydraulic data variability.

Seismo-acoustic data

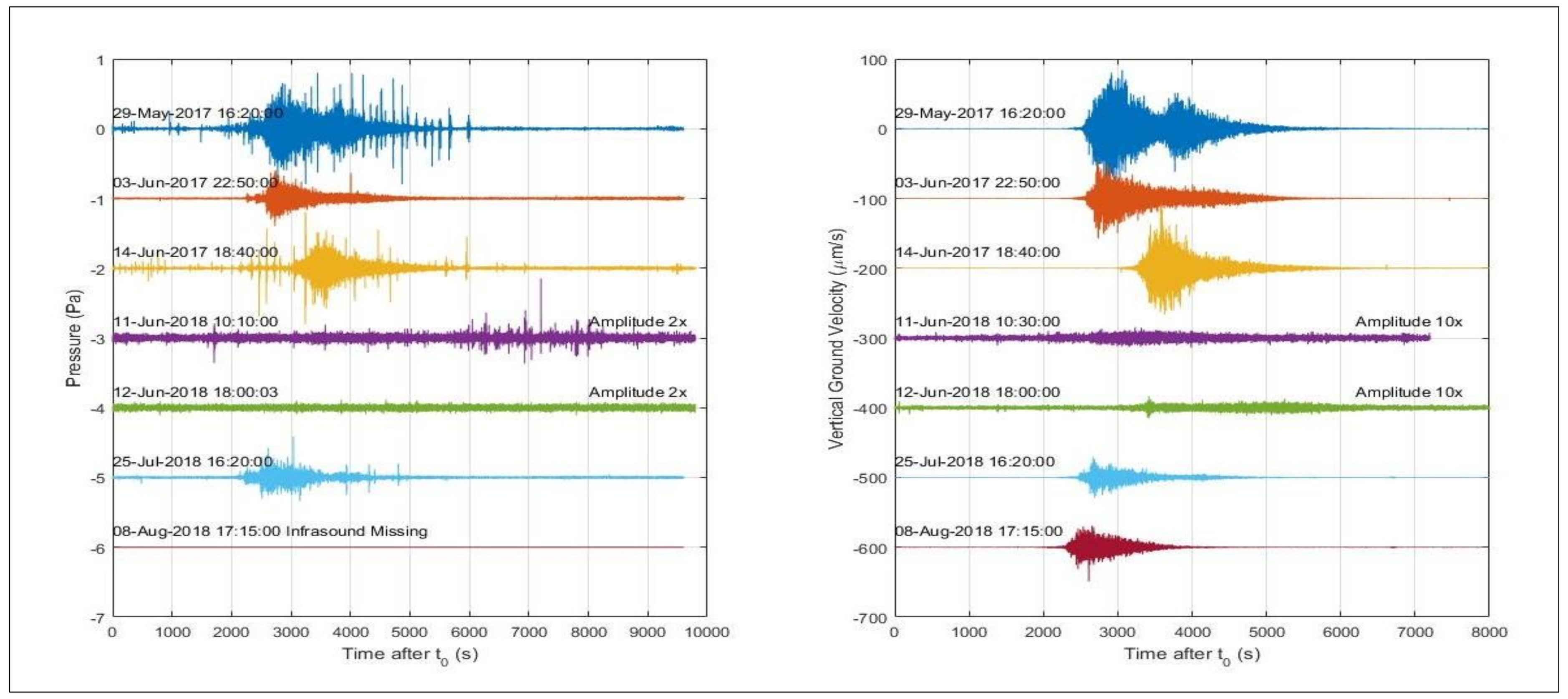

Figure 3: Illgraben 2017-2018 debris-flow events infrasound (left) and seismic (right) waveforms.

Infrasonic and seismic waveforms of debris-flow events occurred at Illgraben respectively in the period 2017-2018 (Figure 3) and in 2019 (Figure 4) typically show an emergent envelope, despite having variable amplitude and duration. In general, seismic signals tend to be clearer than infrasonic ones, with infrasound below the back-ground noise for at least 4 events (Figures 3 and 4; Table 1). It seems thus that debris-flows tend to be more effective as seismic sources than as infrasound sources, especially for smaller debris-flow events.

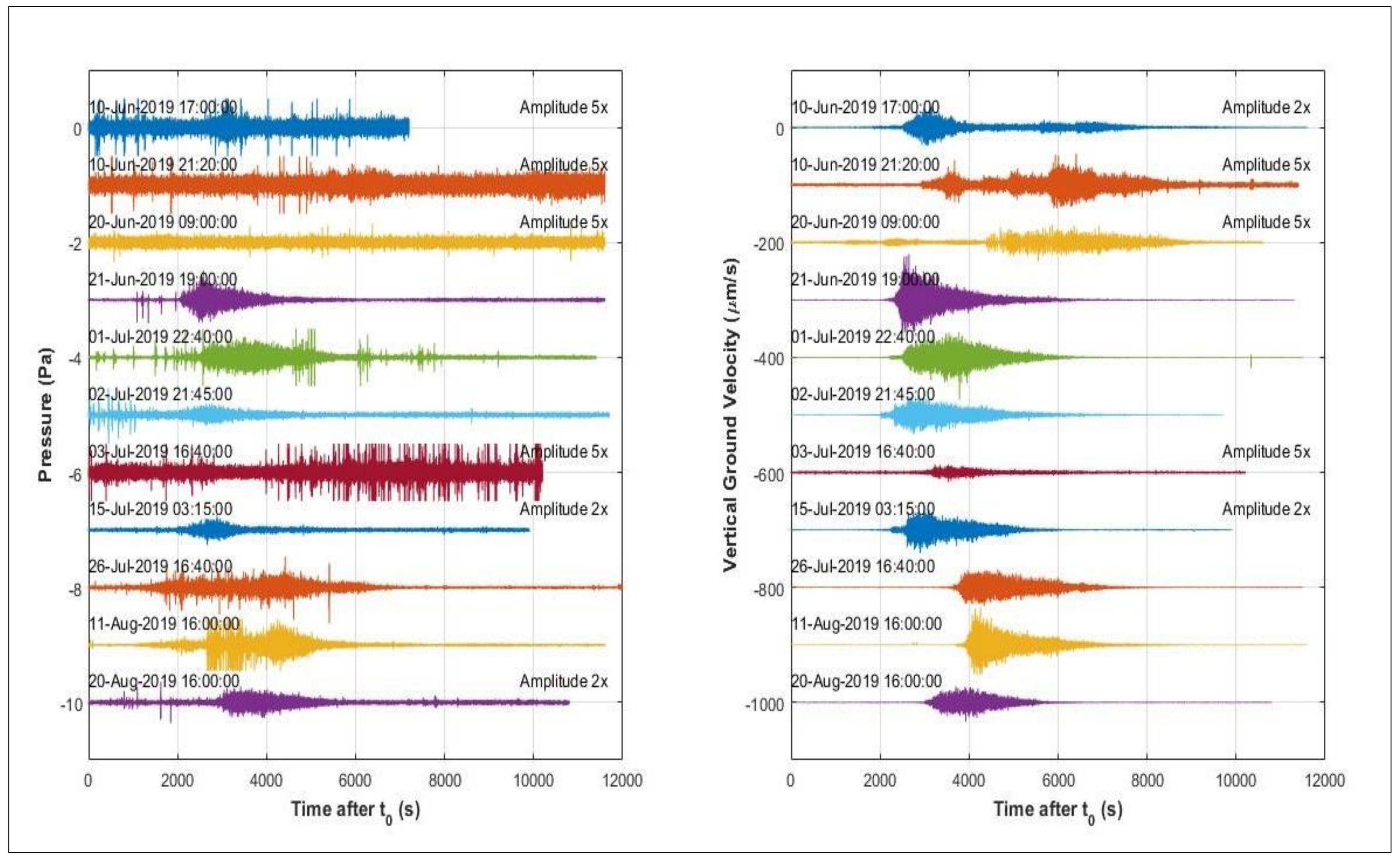

Figure 4: Illgraben 2019 debris-flow events infrasound (left) and seismic (right) waveforms.

Results

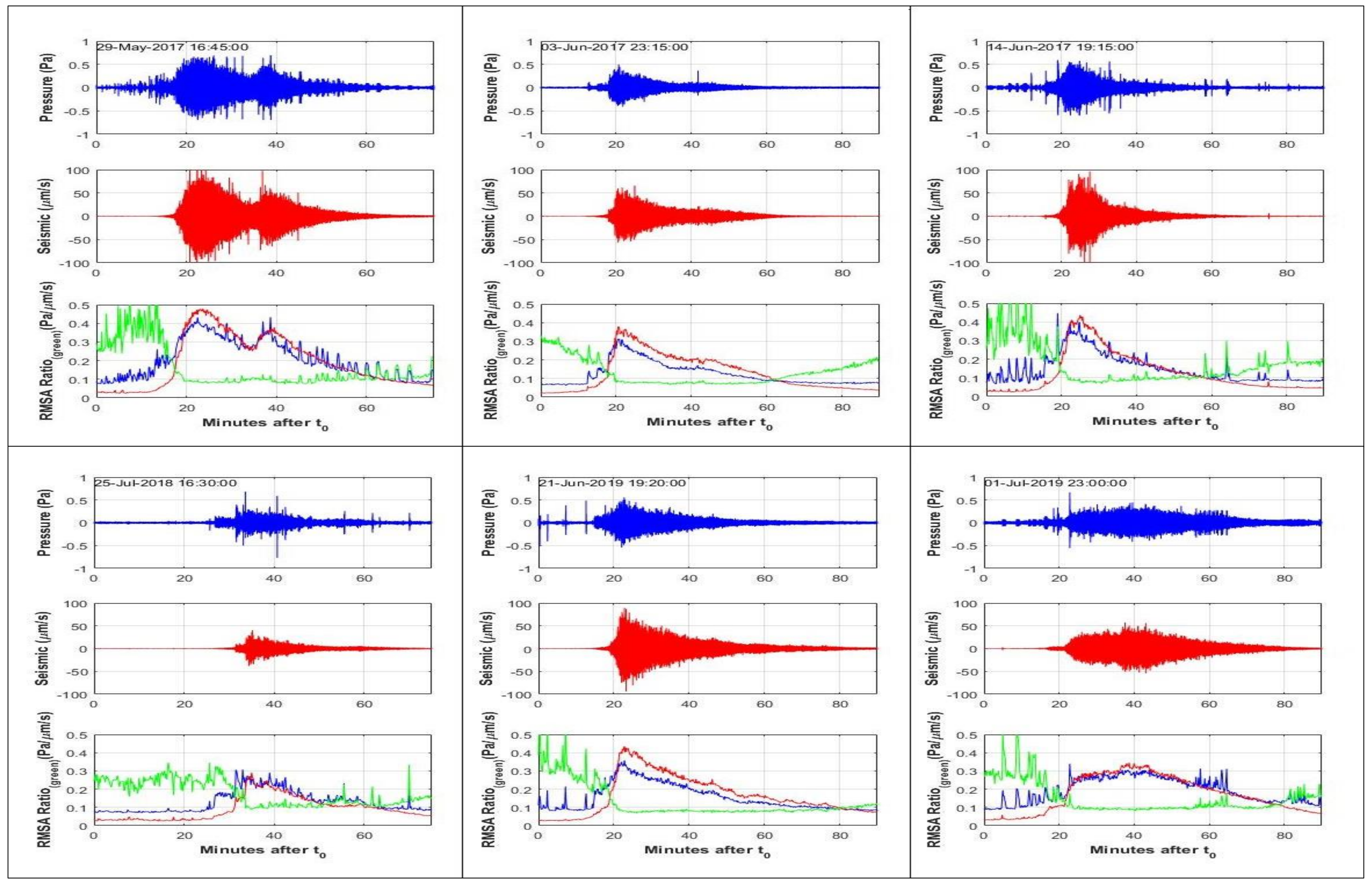

Figure 5: infrasonic (blue) and seismic (red) amplitude analysis of six debris-flow events at Illgraben between 2017 and 2019. The lower diagram in each section shows both infrasonic (blue) and seismic (red) RMSA, together with the ratio (green) between them (y axis values refer to Infrasound-to-Seismic RMSA Ratio). In these diagrams, seismic RMSAs have been divided by a factor of 10.

Infrasonic and seismic RMSA (Root Mean Square Amplitude) computed for 6 of the 18 considered events, is showing a general match between seismic and infrasound, but is showing a variable ratio through time. The infrasound-to-seismic RMSA ratio (the green line) rapidly decreases in the initial phase of the event, indicating that seismic energy radiation grows more effectively than infrasound. After the RMSA peak is reached, the ratio remains constant (≈ 0.1 Pa/μms) during almost all the remaining part of the event, suggesting a stable energy partition between the atmosphere and the ground.

In Figure 6, geophysical data are compared with available hydraulic/physical data. Data show good positive relationships between flow velocity and flow depth with infrasonic and seismic RMSA max amplitude (Figure 6 A). In contrast, a clear relationship between flow density and RMSA values seems to be missing (Figure 6 B). Possibly two opposite trends for lower density (<2000 kg/m^3) and higher density (>2150 kg/m^3) flows might exists, but more data will be required.
From flow velocity and depth, we calculated flow discharge per channel width unit (FD, m^2/s), and combining it with density value we calculated the mass flux per channel width unit (MF, kg/m·s). Comparison with RMSA maximum values (Figure 6C) and RMSA ratio (Figure 6D) is showing a clear linear relationship. These results suggest that the flow discharge is likely controlling seismo-acoustic energy radiation more than the mass flux does. Figure 6D suggests that a discharge increase favors more the infrasonic source mechanisms, probably increasing free surface flow waves number and/or amplitude, than the seismic source mechanisms, whose increase is probably limited by the torrent bed solid boundary.

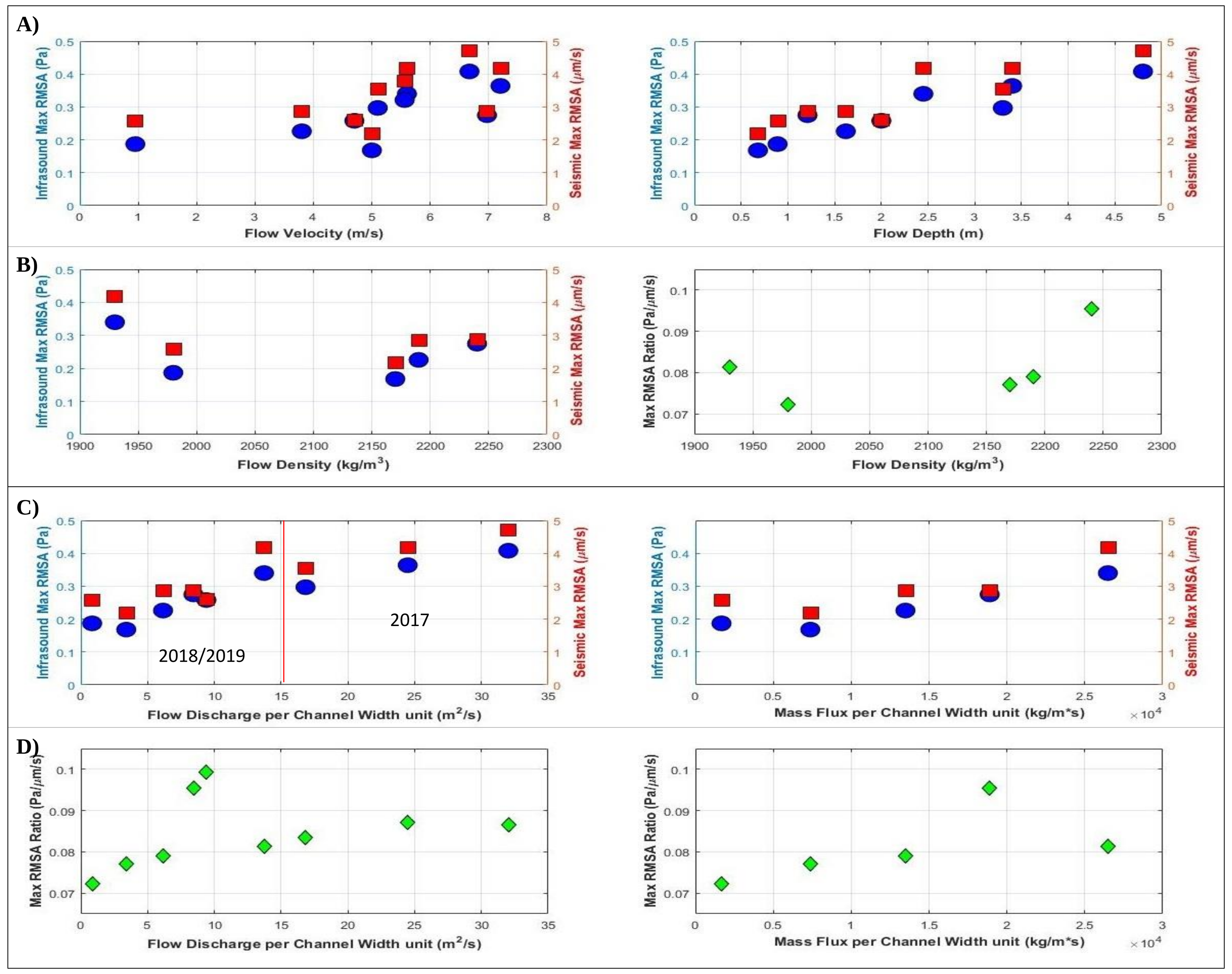

Figure 6: hydraulic-geophysical debris-flows relationships between: A) flow velocity (left) and flow depth (right) and both infrasound (blue circles) and seismic (red squares) max RMSA, B) flow density and both seismic and infrasound max RMSA (left) and the infrasound-to-seismic max RMSA ratio (right), C) discharge (left) and mass flux (right), per channel width unit, and both infrasonic and seismic max RMSA, D) discharge (left) and mass flux (right), per channel width unit, and the infrasound-to-seismic max RMSA ratio.

Concluding remarks

Illgraben debris-flows events are characterized by a stable infrasound-to-seismic RMSA ratio time-trend, reflecting a stable elastic energy partition between atmosphere and ground during the event. Both infrasonic and seismic RMSAs increase with increasing flow velocity and flow depth, while no univocal relation is observed for density. Unit flow discharge and both infrasonic and seismic RMSA are related by a linear positive relation. In addition, an increase in flow discharge leads to an increase of infrasound energy radiation greater than the resulting increase of seismic energy radiation. The role of density (and thus mass flux) on both infrasound and seismic RMSA and on their ratio seems secondary. Being infrasound amplitudes intimately bond to flow discharge, infrasound analysis probably is not the right tool for the study and for the monitoring of smaller debris-flows events.